GMR Genetics and Molecular Research
Online Journal
ISSN:1676-5680

Protective effect of ultrafiltered XinMaiJia extract against H_2O_2-induced injury in human umbilical vein endothelial cells through *NHE1* downregulation

Y.L. Yin[1]*, P. Li[2]*, J. Yang[3]*, D.W. Liu[4]*, R.L. Sun[5], G.P. Pan[2], G.M. Wan[6] and G.R. Wan[2]

[1]School of Basic Medical Sciences, Xinxiang Medical University, Xinxiang, China
[2]College of Pharmacy, Xinxiang Medical University, Xinxiang, China
[3]Puyang City Health School, Puyang, China
[4]Department of Nephrology, The First Affiliated Hospital, Zhengzhou University, Zhengzhou, China
[5]Department of Inspection, Xinxiang Medical University, Xinxiang, China
[6]Ophthalmology, The First Affiliated Hospital, Zhengzhou University, Zhengzhou, China

*These authors contributed equally to this study.
Corresponding author: G.R. Wan
E-mail: guangruiwan@126.com

Genet. Mol. Res. 13 (4): 8436-8449 (2014)
Received August 23, 2013
Accepted June 4, 2014
Published October 20, 2014
DOI http://dx.doi.org/10.4238/2014.October.20.20

ABSTRACT. We examined the protective effects of ultrafiltered XinMaiJia (XMJ) extract in a hydrogen peroxide (H_2O_2)-induced injury model in human umbilical vein endothelial cells (HUVECs) and determined the corresponding changes in the Na^+-H^+ exchanger (NHE1) protein content and *NHE1* gene expression. H_2O_2-induced HUVECs were treated with different concentrations of XMJ extract and the corresponding changes in morphology, activity, membrane permeability, biochemical

indicators, cytokine concentration, NHE1 protein content, and *NHE1* gene expression were determined. H_2O_2 significantly promoted HUVEC injury, whereas ultrafiltered XMJ extract significantly improved the morphological changes in injured HUVECs, increased their activity, and decreased NHE1 gene and protein expression, as well as limited the decrease in membrane permeability and expression of intercellular adhesion molecule-1, vascular cell adhesion molecule-1, interleukin (IL)-1, IL-6, and nuclear factor-κB. Ultrafiltered XMJ extract inhibited H_2O_2-induced HUVEC injury by inhibiting NHE1 activity.

Key words: XMJ; HUVEC; H_2O_2; NHE1

INTRODUCTION

XinMaiJia (XMJ) is a traditional Chinese medicine for treating atherosclerosis (AS), which effectively inhibits the occurrence and development of AS (Wan et al., 2010). XMJ is composed of the following raw materials, by weight: 10-35% functional red kojic rice powder, 1-10% kudzu flavonoid powder, 1-8% soybean isoflavone powder, 1-8% bamboo leaf flavone powder, 1-8% resveratrol powder, 1-6% hawthorne powder, 1-6% *Gastrodia* powder, 1-30% *Auricularia auricula* powder, 0.1-0.2% hippocampus powder, 0.008-0.04% astaxanthin powder, 0.1-0.3% menthol powder, and 20-50% resistant starch.

Vascular endothelial cell injury is the first step in AS development (Arkensteijn et al., 2013). Studies have shown that reactive oxygen species, such as the superoxide anion ($\cdot O^{2-}$), hydroxyl radical ($\cdot OH$), and hydrogen peroxide (H_2O_2), are the major factors that bind as ligands to nuclear receptors in human umbilical vein endothelial cells (HUVECs), participate and regulate the expression of several genes, enhance mononuclear cell adhesion and immigration to the vascular intima, and play a pivotal role in the initial stage of AS, diabetes, hypertension, and heart failure (Yanamoto et al., 2012; Brioschi et al., 2013; Choi et al., 2013; Montoro-García et al., 2013).

The Na^+-H^+ exchangers (NHEs) are a family of membrane-bound ion transport albumins with 9 members (Donowitz et al., 2013; Sasahara et al., 2013). *NHE1* is one of the main housekeeping genes in most eukaryotic cell membranes; it encodes NHE1, which regulates cell pH by exchanging Na^+ with H^+ to maintain a neutral or alkaline pH (Blough et al., 2012; Lin et al., 2012). Studies have shown that NHE1 is involved in several cardiovascular diseases, including AS, hypertension, and heart failure (Lee and Jung, 2012; Vaish and Sanyal, 2012).

To investigate the mechanism of the XMJ-induced inhibition of AS occurrence and development, we studied HUVECs under H_2O_2 stress. Ultrafiltered XMJ extract was used for HUVECs treated with H_2O_2, and NHE1 protein expression was detected using Western blot analysis, immunofluorescence, and immunohistochemistry. *NHE1* gene expression in HUVECs was examined using fluorescence quantification polymerase chain reaction (PCR).

MATERIAL AND METHODS

Drugs and chemicals

The XMJ crude drug was purchased from Beijing Tong Ren Tang Co. (Beijing, Chi-

na). Lovastatin and H_2O_2 were purchased from Sigma (St. Louis, MO, USA). Rabbit anti-NHE1 polyclonal antibodies, horseradish peroxidase-labeled goat anti-rabbit IgG antibodies, and Cy3-labeled goat anti-rabbit IgG antibodies were purchased from Chemicon (Temecula, CA, USA). The test kits for malondialdehyde (MDA), superoxide dismutase (SOD), nitric oxide (NO), interleukin (IL)-1, IL-6, intercellular cell adhesion molecule (ICAM)-1, vascular cell adhesion molecule (VCAM)-1, matrix metalloproteinase (MMP)-2, tissue inhibitor of metalloproteinase (TIMP)-2, and nuclear factor-κB were purchased from R&D Systems (Minneapolis, MN, USA). Other reagents were of analytical grade and purchased in China.

Ultrafiltration membrane extracts prepared from XMJ

One thousand grams of XMJ crude drug was placed into a container with 6000 mL water and heated for 1 h in a microwave oven at 1000 W. The mixture was filtered through a 4-gauze filter to obtain the liquid extract. The extraction was repeated using 6000 mL water to produce 2 XMJ solutions that were filtered using sterile absorbent cotton. We ultrafiltered the XMJ water decoction at a pressure of 0.5 kPa/m^3, temperature of 25°C, and flow rate of 100 $L \cdot h^{-1} \cdot m^{-2}$. Next, 5000 mL filtrate was concentrated to 1000 mL, equivalent to 1 g/mL XMJ. The XMJ stock solution was stored in a refrigerator at 4°C.

Cell experiment

HUVECs purchased from the American Type Culture Collection (ATCC, Manassas, VA, USA) were routinely maintained in phenol red-stained Dulbecco's modified Eagle's medium supplemented with 15% newborn calf serum, 100 U/mL penicillin, and 0.1 mg/L phytomycin in a 37°C incubator containing 5% CO_2. Third-generation HUVECs were used in subsequent experiments. The cells were randomly divided into 8 groups and incubated for 24 h with the corresponding drugs indicated below. Cells in the first group were incubated with Kreb's solution as a blank control (N = 6). Cells in the second group were incubated with 500 mg/L XMJ as the XMJ control group (N = 6). Cells in the third group were incubated with 200 μM H_2O_2 as the model group (N = 6). Cells in the fourth group were incubated with 1 μM lovastatin and 200 μM H_2O_2 as the lovastatin group (N = 6). Cells in the fifth group were incubated with 50 μM zhibituo and 200 μM H_2O_2 as the zhibituo group (N = 6). Cells in the sixth group were incubated with 25 μM XMJ and 200 μM H_2O_2 as the low-dose XMJ group (N = 6). Cells in the seventh group were incubated with 50 μM XMJ and 200 μM H_2O_2 as the middle-dose XMJ group (N = 6). Cells in the eighth group were incubated with 100 μM XMJ and 200 μM H_2O_2 as the high-dose XMJ group (N = 6). After treatment, cultured cells were collected for subsequent analysis.

Hematoxylin and eosin (HE) staining

The cells grew along the walls of the bottle in each experimental group. The supernatant on the 6-well plate was discarded and the cells were washed 3 times with phosphate-buffered saline (PBS), pH 7.4. The cells were soaked in 95% ethanol for 20 min and washed twice with PBS. Hematoxylin was used to dye the cells for 2-3 min and the cells were washed with pure water. Once the nuclei were deeply stained, 1% hydrochloric acid alcohol solution was used to carry out color separations for 5 s and then the samples were washed with pure water.

The mixture was dehydrated with 70% alcohol for 10 min followed by 90% alcohol for another 10 min, and then washed with distilled water and stained with alcoholic eosin for 2-3 min.

HUVEC activity detection

When the cell concentration reached 10^6 cells/cm^2, the cells were washed twice with PBS and mixed with 0.25% trypsin. The flasks were shaken while the nozzle was blown to detach the cells from the wall of the bottle. Next, 1 g/L 5% thiophene azole blue solution was added into each well at 37°C. Finally, 10 μL cell suspension was analyzed on an automatic cell counting board (Countstar, Inno-Alliance Biotech, USA) to determine viability, average density, and aggregation rates of the cells in each group.

HUVEC membrane permeability determination

The HUVEC membrane permeability was determined following protocols described in Postlethwaite et al. (1976) and Ding et al. (1993). The osmotic reflection coefficient (σ) was calculated using the following formula: endothelial membrane filtration coefficient (Kf) ($\mu L \cdot min^{-1} \cdot cm^{-2} \cdot kPa^{-1}$) = $JV/(\Delta p - \sigma \cdot \Delta \pi)$, where $\sigma = 1 - C_F/C_P$ and π (kPa) = C (mosm·L^{-1})·2.6 (kPa·L·mosm^{-1}), and C_P is the upper chamber white protein concentration, C_F is the inferior vena albumin concentration, C is the albumin milli seepage quantity concentration, Δp is the perfusion pressure, and π is the colloid osmotic pressure.

HUVEC cell supernatant fluid biochemical indicator detection

Cells were grown on 6-well plates at 2 mL per well and were treated as described above and then analyzed. The supernatant fluid was detected using a biochemical indicator. The culture fluid was collected to measure SOD, MDA, and NO activity as described in the corresponding kits.

Enzyme-linked immunosorbent assay (ELISA)

The cells were inoculated on 6-well plates at 2 mL per well and were treated as described above. The supernatant fluid was collected from various wells and the optical density (OD) of each well was determined at a wavelength of 450 nm according to the ELISA kit instructions. We used the absorbance as the ordinate and the standard concentration of the liquid in the reagent box as the abscissa. We also determined the relevant curve and calculated its equation. The concentrations of IL-1, IL-6, ICAM-1, and VCAM-1 were calculated by substituting the OD values of the samples into the equation of the standard curve.

Western blot analysis

The cells were allowed to grow on the walls of the bottles in each experimental group. The supernatant from the 6-well plates was discarded and the cells were washed 3 times with PBS, pH 7.4. Next, precooled cell lysates were added and the protein concentration was determined using the bicinchoninic acid method. Finally, HUVEC NHE1 protein expression was determined in each experimental group.

Immunohistochemical method

Cells were soaked in 95% ethanol for 20 min and then washed twice with PBS for 1 min. The cells were sealed with animal serum, after which phosphorylated rabbit anti-NHE1 at l:500 dilution was added. The mixture was stored overnight at 4°C. Horseradish peroxidase-labeled goat anti-rabbit IgG and enzymes were added as chromogenic agents. The cells were stained with Mayer hematoxylin and dehydrated using an alcohol gradient. Cells were clarified with xylene and mounted onto slides using neutral gum. Finally, the specimens were observed and photographed under a microscope and the images were processed and analyzed using the Image Analysis software to determine the OD.

Immunofluorescence

The supernatant was discarded from the 6-well plates and 0.01 M PBS, pH 7.4, was added to the specimen sheet for testing. The PBS was discarded after 10 min and the moisture of the specimen was maintained. Phosphorylated rabbit anti-NHE1 at l:200 dilution was added, and the cells were incubated overnight at 4°C. The membrane was washed 3 times with Tris-buffered saline containing Tween 20, and an antibody dilution solution (1:1000) containing Cy3-labeled goat anti-rabbit IgG was added. The cells were covered completely in an enamel box with a lid and incubated for 30 min. The slides were removed from the enamel box and washed with 0.01 M PBS, pH 7.4, then, soaked in the liquid containing 0.01 M PBS, pH 7.4 for 3 times, and placed on shelves. We processed and analyzed OD using the Image Analysis software.

Real-time quantitative fluorescence

Total cellular RNA was extracted using a TRIzol reagent kit. Primers were synthesized by Takara Biotechnology Dalian Co., Ltd. (TaKaRa, Shiga, Japan). The forward and reverse primer sequences were as follows (5' to 3'): e1: GAGCTGAAACAAGCCAT TGA, e2: AACGGTCTGTTGGTTTAGCC. The reaction included 10 μL: 5 μL 2X SYBR Premix Taq reaction buffer, 0.25 μL 10 μM PCR forward primer, 0.25 μL 10 μM PCR reverse primer, 0.5 μL cDNA template, and 4 μL deionized water. The melting curve ranged from 60° to 95°C. After the reaction, the PCR samples were separated via agarose gel electrophoresis to verify whether the fragment had been amplified. After quantitative PCR, the data were analyzed using the PikoReal Software 2.1. We calculated the corresponding Ct values after adjusting the baseline cycle threshold through the requirements of the software.

Statistical analysis

All data are reported as means ± standard error. We analyzed the data using single-factor variance and SNK-q multiple comparison for comparisons between different groups. This comparison was accomplished using the SPSS 13.0 statistical software (SPSS, Inc., Chicago, IL, USA) and differences with $P < 0.05$ were considered to be statistically significant.

RESULTS

Protective effect of XMJ against H_2O_2-induced injury in HUVECs

HE-stained HUVECs were observed under a microscope (400X): HUVEC apoptosis was significantly reduced in the high-dose XMJ group. Cytoplasmic staining was relatively uniform and the metachromatic particles of the nucleus were not clearly observed. The cells were arranged closely and their morphology was normal. The XMJ-treated cells clearly differed from the model group. Higher doses of XMJ exhibited a significant protective effect against H_2O_2-induced injury in HUVECs; lovastatin and zhibituo also protected HUVECs against H_2O_2-induced injury. However, the protective effects of lovastatin and zhibituo were relatively weaker than that of high-dose XMJ, based on morphological differences. The protective effects of low- and middle-dose XMJ against H_2O_2-induced injury in HUVECs were significantly weaker than that of high-dose XMJ (Figure 1A-H).

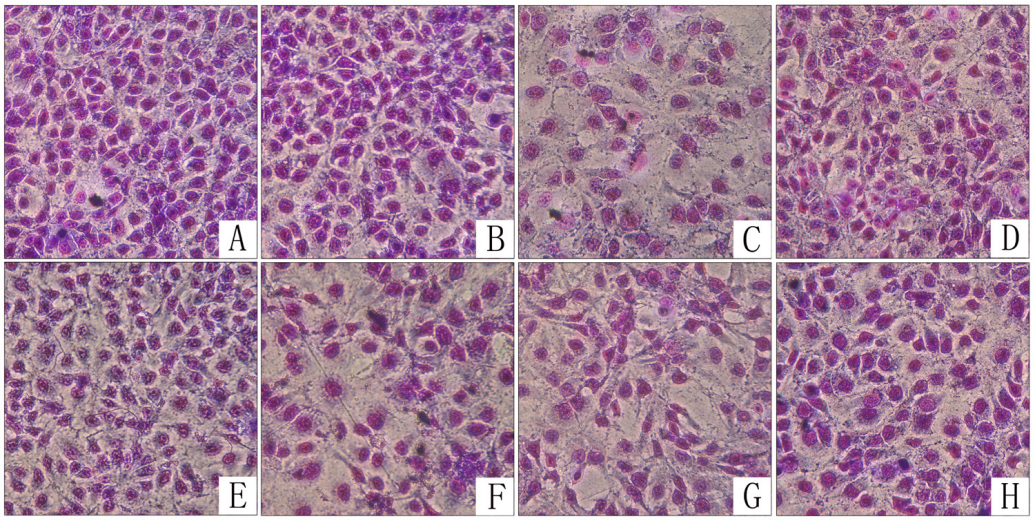

Figure 1. Protective effect of XMJ on HUVEC injury induced by H_2O_2 at 400X magnification (HE stain). **A.** Blank control group. **B.** XMJ control group. **C.** Model group. **D.** Lovastatin group. **E.** Zhibituo group. **F.** Low-dose XMJ group. **G.** Middle-dose XMJ group. **H.** High-dose XMJ group.

Effect of XMJ on HUVEC cell activity

In the high-dose XMJ group, activity of HUVEC cells was 89.54%, whereas the average degree of compaction was 0.77 and the rate of polymerization was 60.83% (Figure 2H). In the model group, HUVEC activity was 54.13%, the average degree of compaction was 0.78 and the rate of polymerization was 52.52% (Figure 2C). The HUVEC activity rate following treatment with high-dose XMJ was significantly higher compared with the model group ($P < 0.05$). High-dose XMJ exhibited a significant protective effect against H_2O_2-induced inhibition of HUVEC activity. Lovastatin and zhibituo significantly protected against H_2O_2-induced

inhibition of HUVEC activity (Figure 2D and E). The XMJ groups significantly differed from the model group ($P > 0.05$). The high-dose XMJ group did not significantly differ from the lovastatin with zhibituo group regarding HUVEC activity. The protective effects of low- and middle-dose XMJ against H_2O_2-induced inhibition of HUVEC activity were significantly weaker than that of high-dose XMJ (Figure 2F, G, and H); thus, the effects of XMJ were dose-dependent. However, the differences in the average degree of compaction and rate of polymerization did not significantly differ among the low-, middle-, and high-dose XMJ groups ($P > 0.05$; Figure 2F, G, and H).

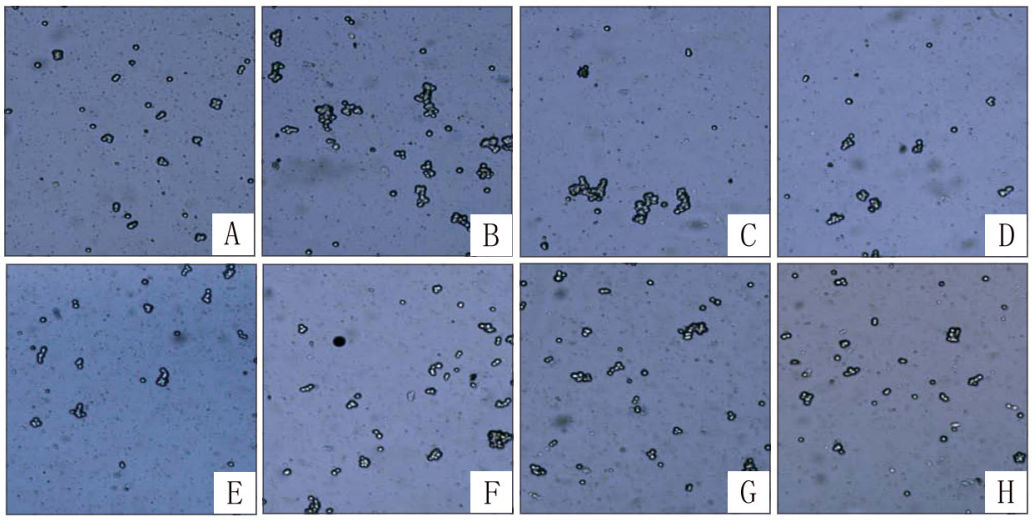

Figure 2. Countstar automatic cell counter detects the effect of XMJ on HUVEC cell activity. **A.** Blank control group. **B.** XMJ control group. **C.** Model group. **D.** Lovastatin group. **E.** Zhibituo group. **F.** Low-dose XMJ group. **G.** Middle-dose XMJ group. **H.** High-dose XMJ group.

Protective effects of XMJ on the H_2O_2-induced decrease in permeability of HUVEC membrane

The Jv value of the HUVECs was 29.43 ± 7.53 $\mu L \cdot min^{-1} \cdot cm^{-2}$, the Kf value was 12.43 ± 2.24 $\mu L \cdot min^{-1} \cdot cm^{-2} \cdot kPa^{-1}$, and the σ value was 0.59 ± 0.08. In the model group, the Jv value of the HUVECs was 44.47 ± 8.56 $\mu L \cdot min^{-1} \cdot cm^{-2}$, the Kf value was 17.66 ± 3.43 $\mu L \cdot min^{-1} \cdot cm^{-2} \cdot kPa^{-1}$, and the σ value was 0.29 ± 0.03. The Jv value of the HUVECs in the high-dose XMJ group was significantly decreased compared with that of the model group. The Kf value also decreased, whereas the σ value significantly increased ($P < 0.05$). These results indicate that high-dose XMJ protects against the decrease in H_2O_2-induced permeability of the HUVEC membrane. Lovastatin and zhibituo also significantly protected against the H_2O_2-induced decrease in the permeability of the HUVEC membrane compared with the model group ($P < 0.05$). The protective effects of high-dose XMJ were stronger than those of lovastatin and zhibituo groups ($P < 0.05$). The protective effects of low- and middle-dose XMJ against the H_2O_2-induced decrease in the permeability of the HUVEC membrane were significantly weaker than that of high-dose XMJ ($P < 0.05$); thus, the effect was dose-dependent (Table 1).

Table 1. Protective effects of XMJ on declination of the permeability of HUVEC monolayer induced by H_2O_2.

Group	Jv (μL·min^{-1}·cm^{-2})	Kf (μL·min^{-1}·cm^{-2}·kpa^{-1})	σ
Blank control group	27.26 ± 4.63*#	11.34 ± 2.87*#	0.54 ± 0.07*#
XMJ control group	28.43 ± 5.35*#	11.54 ± 2.89*#	0.55 ± 0.07*#
Model group	44.47 ± 8.56#△	17.66 ± 3.43#△	0.29 ± 0.03#△
Lovastatin group	33.45 ± 6.49*#△	14.46 ± 2.98*#△	0.38 ± 0.07*#△
Zhibituo group	35.32 ± 5.12*#△	14.64 ± 2.39*#△	0.43 ± 0.06*#△
Low-dose XMJ group	34.34 ± 5.43*#△	14.54 ± 2.32*#△	0.41 ± 0.08*#△
Middle-dose XMJ group	30.12 ± 5.67*#△	12.28 ± 2.13*#△	0.46 ± 0.08*#△
High-dose XMJ group	29.43 ± 7.53*△	12.43 ± 2.24*△	0.59 ± 0.08*△

Data are reported as means ± SE for N = 6 in each group. *P < 0.05 *vs* model group; #P < 0.05 *vs* high-dose XMJ group; △P < 0.05 *vs* blank control group.

Effect of XMJ on the SOD and MDA content of HUVEC supernatant under H_2O_2 induction

The mean SOD content was 18.21 ± 1.39 U/mL and the MDA content was 1.37 ± 0.26 μM. In the model group, the SOD content was 6.35 ± 0.87 U/mL and the MDA content was 1.84 ± 0.26 μM. SOD and MDA contents following XMJ treatment significantly differed from those of the model group (P < 0.05). The SOD content significantly increased, while the MDA content decreased following high-dose XMJ treatment. Lovastatin and zhibituo clearly suppressed the decrease in SOD content and increase in MDA content of the HUVEC supernatant under H_2O_2 induction, which significantly differed from values in the model group (P < 0.05). The SOD and MDA contents in the HUVEC supernatant in the lovastatin with zhibituo treatment group did not significantly differ from those in the model group (P > 0.05). Suppression of the H_2O_2-induced decrease in SOD content and the H_2O_2-induced increase in MDA content of the HUVEC supernatant in the low- and middle-dose XMJ treatment groups were significantly weaker than those in the high-dose XMJ treatment group (P < 0.05), once again demonstrating that the effect of XMJ was dose-dependent (Figure 3).

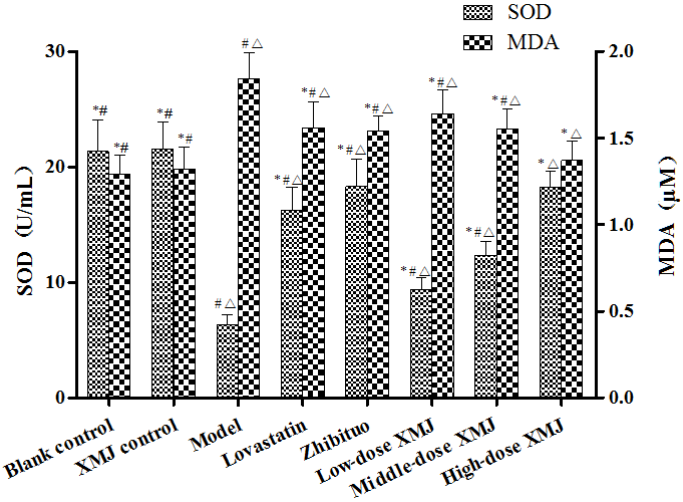

Figure 3. Effect of XMJ on supernatant superoxide dismutase (SOD) and malondialdehyde (MDA) contents in HUVECs induced by H_2O_2. *P < 0.05 *vs* model group; #P < 0.05 *vs* high-dose XMJ group; △*P < 0.05 *vs* blank control group.

Effect of XMJ on cytokine concentrations in HUVEC supernatant under H_2O_2 induction

In the middle-dose XMJ group, the ICAM-1, VCAM-1, IL-1, and IL-6 concentrations were 36.33 ± 7.32 ng/L, 36.66 ± 1.58 μg/L, 14.75 ± 2.04 ng/L, and 6.05 ± 0.84 ng/L, respectively. In the model group, the ICAM-1, VCAM-1, IL-1, and IL-6 concentrations were 71.18 ± 6.67 ng/L, 44.81 ± 2.09 μg/L, 18.34 ± 2.14 ng/L, and 7.24 ± 0.92 ng/L, respectively. Lovastatin and zhibituo significantly suppressed the increase in ICAM-1, VCAM-1, IL-1, and IL-6 ($P < 0.05$) compared with the model group. Cytokine concentrations in the HUVEC supernatant from the lovastatin and zhibituo groups did not significantly differ from that of the middle-dose XMJ group ($P > 0.05$). Low-dose XMJ suppressed the H_2O_2-induced increase in ICAM-1, VCAM-1, IL-1, and IL-6 to a lesser extent than the middle-dose XMJ group ($P < 0.05$). However, high-dose XMJ also suppressed the H_2O_2-induced increase in ICAM-1, VCAM-1, IL-1, and IL-6 to a lesser extent than middle-dose XMJ (Table 2).

Table 2. Effect of XMJ on supernatant cytokines of HUVECs induced by H_2O_2 (N = 6, mean ± SE).

Group	ICAM-1 (ng/L)	VCAM-1 (μg/L)	IL-1 (ng/L)	IL-6 (ng/L)
Blank control group	28.91 ± 3.65*#	36.49 ± 1.22*#	14.23 ± 1.25*#	5.93 ± 0.45*#
XMJ control group	36.33 ± 4.39*#	38.78 ± 2.39*#	13.93 ± 1.36*#	6.51 ± 0.65*#
Model group	71.18 ± 6.67#Δ	44.81 ± 2.09#Δ	18.34 ± 2.14#Δ	7.24 ± 0.92#Δ
Lovastatin group	38.55 ± 4.16*Δ	35.84 ± 1.96*Δ	14.63 ± 1.57*Δ	6.05 ± 0.78*Δ
Zhibituo group	34.10 ± 4.12*Δ	36.49 ± 2.68*Δ	14.79 ± 1.69*Δ	6.19 ± 0.65*Δ
Low-dose XMJ group	62.78 ± 5.47*#Δ	38.94 ± 2.47*#Δ	15.49 ± 2.31*#Δ	6.48 ± 0.77*#Δ
Middle-dose XMJ group	36.33 ± 7.32*Δ	36.66 ± 1.58*Δ	14.75 ± 2.04*Δ	6.05 ± 0.84*Δ
High-dose XMJ group	39.29 ± 4.57*#Δ	43.38 ± 2.39*#Δ	16.07 ± 2.55*#Δ	7.21 ± 0.98*#Δ

*$P < 0.05$ *vs* model group; #$P < 0.05$ *vs* middle-dose XMJ group; Δ$P < 0.05$ *vs* blank control group.

Western blot analysis of NHE1 content of HUVECs

The NHE1/β-actin ratio was 0.64 ± 0.09 in the high-dose XMJ group, whereas it was 2.23 ± 0.02 in the model group. The NHE1/β-actin ratio in the high-dose XMJ was significantly higher than in the model group ($P < 0.05$). Lovastatin and zhibituo significantly suppressed the H_2O_2-induced decrease in NHE1 content in HUVECs ($P < 0.05$). High-dose XMJ significantly suppressed the H_2O_2-induced decrease in NHE1 content in HUVECs more than those observed in the lovastatin and zhibituo treatment groups ($P < 0.05$). The NHE1/β-actin ratios of the low- and middle-dose XMJ groups were significantly lower than that of high-dose XMJ treatment group ($P < 0.05$; Figure 4).

Immunohistochemical detection of NHE1 protein content of HUVECs

The degree of NHE1 staining saturation in the high-dose XMJ treatment group was 15.69 ± 0.78%, chromaticity was 32.69 ± 2.33, grayscale was 187.65 ± 14.33, red was 132.65 ± 10.27, green was 152.79 ± 11.29, and blue was 142.39 ± 11.57 (Figure 5H). The degree of NHE1 staining saturation in the model group was 7.11 ± 0.39%, chromaticity was 44.21 ± 4.28, grayscale was 251.06 ± 10.27, red was 153.33 ± 13.37, green was 177.12 ± 1 4.27, and blue was 163.27 ± 10.24 (Figure 5C). The NHE1 coloration index of the high-dose XMJ group significantly differed from that of the model group ($P < 0.05$). Lovastatin and zhibituo treat-

ment significantly affected the H_2O_2-induced NHE1 coloration index of HUVECs (Figure 5D and E) compared with the model group ($P < 0.05$). HUVEC NHE1 staining indicated that the effect of high-dose XMJ on H_2O_2-induced stress was greater than those of lovastatin and zhibituo treatment ($P < 0.05$). The effect of low- and middle-dose XMJ on the NHE1 coloration index of HUVECs under H_2O_2 induction was significantly weaker than that of high-dose XMJ treatment as the effect of XMJ was dose-dependent (Figure 5F, G, and H).

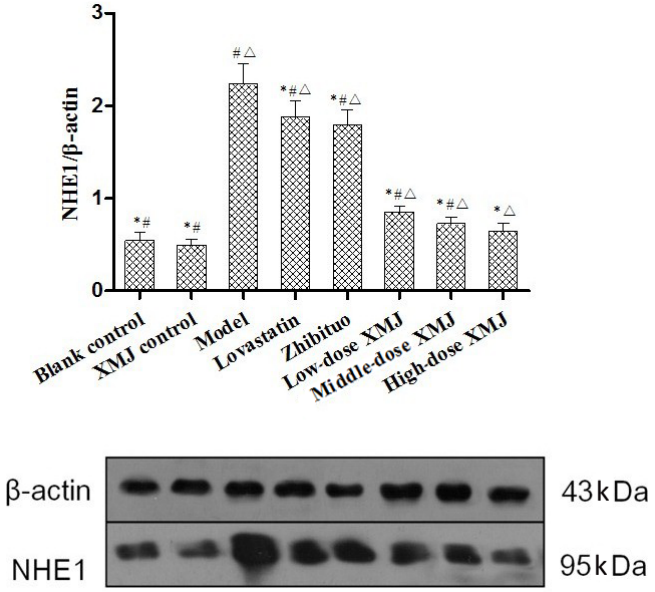

Figure 4. Western blotting to detect expression of the NHE1 protein in HUVECs. *P < 0.05 *vs* model group; #P < 0.05 *vs* high-dose XMJ group; ΔP < 0.05 *vs* blank control group.

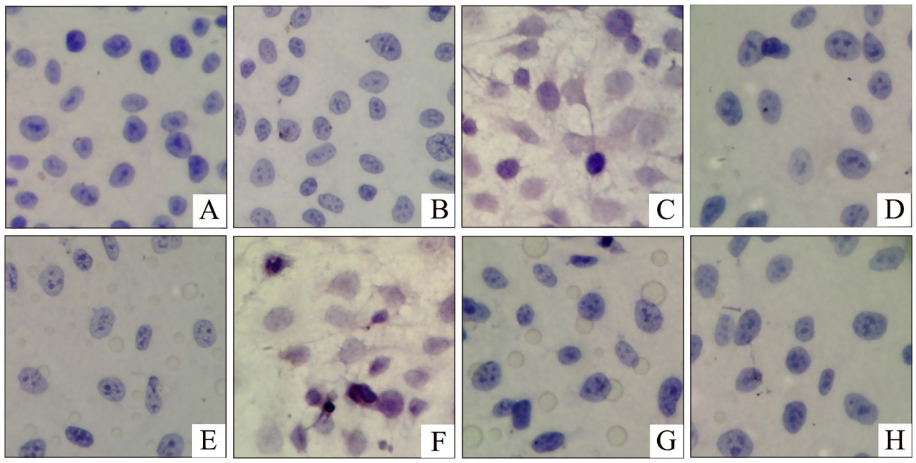

Figure 5. Immunohistochemical detection of NHE1 protein expression in HUVECs (400X). **A.** Blank control group. **B.** XMJ control group. **C.** Model group. **D.** Lovastatin group. **E.** Zhibituo group. **F.** Low-dose XMJ group. **G.** Middle-dose XMJ group. **H.** High-dose XMJ group.

Immunofluorescence assay of NHE1 content in HUVECs

NHE1 was primarily expressed in the cytoplasm of the HUVECs; positive signals were diffused in the yellowish-green spectrum. The fluorescence intensity of NHE1 was 69.66 ± 5.34 in the high-dose XMJ treatment group (Figure 6H), whereas in the model group it was 172.54 ± 12.37 (Figure 6C). The fluorescence intensity of the high-dose XMJ group was significantly higher than that of the model group ($P < 0.05$). Lovastatin and zhibituo treatment significantly increased the fluorescence intensity of NHE1 in the HUVECs under H_2O_2 induction compared with the model group (Figure 6D and E; $P < 0.05$). The fluorescence intensity of NHE1 in the HUVECs treated with high-dose XMJ was greater than that of lovastatin and zhibituo treatment ($P < 0.05$). The fluorescence intensity of NHE1 in the HUVECs treated with low- and middle-dose XMJ was clearly weaker than that treated with high-dose XMJ ($P < 0.05$); the effect of XMJ was dose-dependent (Figure 6F, G, and H).

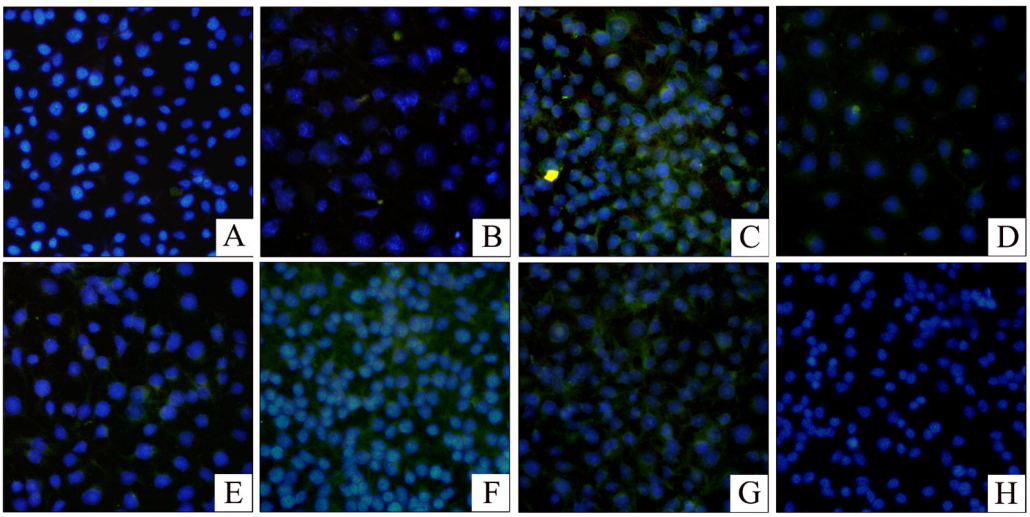

Figure 6. Immunofluorescence detection of expression of the NHE1 protein in HUVECs (400X). **A.** Blank control group. **B.** XMJ control group. **C.** Model group. **D.** Lovastatin group. **E.** Zhibituo group. **F.** Low-dose XMJ group. **G.** Middle-dose XMJ group. **H.** High-dose XMJ group.

Fluorescence quantitative-PCR to detect the *NHE1* gene in HUVECs

The fluorescence intensity of the *NHE1*/*GAPDH* genes was 1.12 ± 0.22 in the high-dose XMJ group and 4.98 ± 0.87 in the model group. The fluorescence intensity in the high-dose XMJ group was significantly higher than that in the model group ($P < 0.05$). The fluorescence intensity of the *NHE1* gene in HUVECs under H_2O_2 induction in the lovastatin and zhibituo groups was significantly higher than that in the model group ($P < 0.05$). The fluorescence intensity of the *NHE1* gene in HUVECs treated with high-dose XMJ was greater than that in cells treated with lovastatin and zhibituo ($P < 0.05$). The fluorescence intensities of the *NHE1* gene in the HUVECs treated with low- and middle-dose XMJ were clearly weaker than that following high-dose XMJ treatment ($P < 0.05$); the effects of XMJ were therefore dose-dependent (Figure 7).

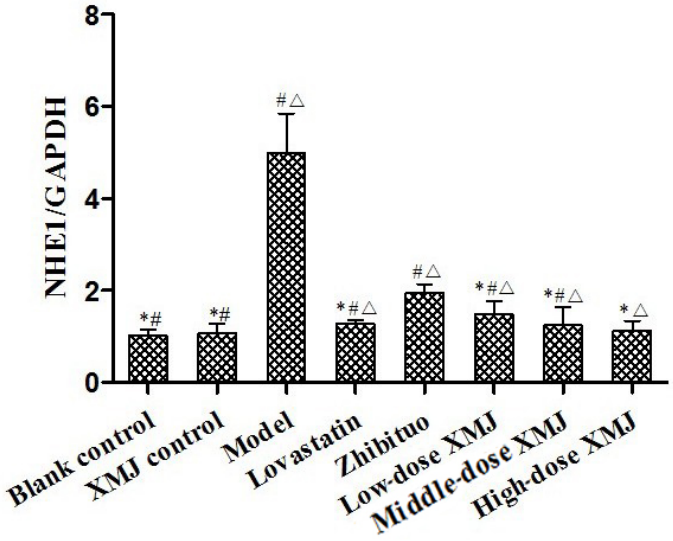

Figure 7. Fluorescence quantitative-PCR to detect gene expression of *NHE1* in HUVECs. *P < 0.05 *vs* model group; #P < 0.05 *vs* high-dose XMJ group; △P < 0.05 *vs* blank control group.

DISCUSSION

The cell membrane ion exchange protein NHE1 is a transmembrane protein present in all eukaryotic cells that regulates intracellular pH by exchanging Na^+ and H^+ (Loo et al., 2012). A previous study showed that NHE1 maintains the neutral to slightly basic internal environment of the human body (Xiang et al., 2012). The human *NHE1* gene is located on chromosome 1p35-36; the cDNA has a total length of 5 kb with a 2445-bp open reading frame. The NHE1 protein has a molecular mass of 100 x 10^3 and is composed of 815-amino acid residues. The hydrophobic N-terminal is the functional domain that mediates Na^+ influx and H^+ efflux, whereas the hydrophilic C-terminal adjusts intracellular pH (Czepán et al., 2012).

The stress factor H_2O_2 used in this study is a powerful oxidant (Pan et al., 2013). In the experiment, the MDA content increased as the SOD content decreased, indicating that oxygenation damaged the HUVECs. Cytokines such as IL-1, IL-6, ICAM-1, and VCAM-1 are highly expressed by HUVECs under oxidative stress (Sánchez Rodríguez et al., 2013), which is consistent with our results. This study showed that cytokines promote cell multiplication by activating NHE1. Our results showed that H_2O_2 damages HUVECs, reduces HUVEC activity, increases membrane permeability, and upregulates NHE1 gene and protein expression. Overall, the results indicated that H_2O_2-induced NHE1 expression damaged the HUVECs.

Increased NHE1 activity decreases the activity of the Na^+-K^+-ATP system in the cell membrane, increasing the intracellular Na^+ concentration and further increasing the intracellular Ca^{2+} concentration through bidirectional Na^+/Ca^{2+} exchange to result in intracellular Ca^{2+} overload (Mo et al., 2011). Ca^{2+} overload disrupts mitochondrial function, reduces cellular anti-oxidant capacity, and degrades membrane phospholipids by activating phosphatase, which induces organelle disorganization, cellular swelling, apoptosis, and death (Nagata et al., 2011).

We found that XMJ dose-dependently inhibited NHE1 expression, protected HUVECs against damage, limited the decrease in HUVEC activity, and limited the increase in HUVEC membrane permeability. These results indicate that XMJ protects HUVECs by inducing NHE1 activity, which has therapeutic applications for the treatment of AS, heart failure, coronary artery disease, hypertension, and tumors.

ACKNOWLEDGMENTS

Research supported by the Department of Science and Technology of Henan Province of China (#121100910300).

REFERENCES

Arkensteijn BW, Berbée JF, Rensen PC, Nielsen LB, et al. (2013). The apolipoprotein m-sphingosine-1-phosphate axis: biological relevance in lipoprotein metabolism, lipid disorders and atherosclerosis. *Int. J. Mol. Sci.* 14: 4419-4431.

Blough MD, Al-Najjar M, Chesnelong C, Binding CE, et al. (2012). DNA hypermethylation and 1p Loss silence NHE-1 in oligodendroglioma. *Ann. Neurol.* 71: 845-849.

Brioschi M, Lento S, Tremoli E and Banfi C (2013). Proteomic analysis of endothelial cell secretome: a means of studying the pleiotropic effects of Hmg-CoA reductase inhibitors. *J. Proteomics* 78: 346-361.

Choi S, Park MS, Lee YR, Lee YC, et al. (2013). A standardized bamboo leaf extract inhibits monocyte adhesion to endothelial cells by modulating vascular cell adhesion protein-1. *Nutr. Res. Pract.* 7: 9-14.

Czepán M, Rakonczay Z Jr, Varro A, Steele I, et al. (2012). NHE1 activity contributes to migration and is necessary for proliferation of human gastric myofibroblasts. *Pflugers Arch.* 463: 459-475.

Ding ZQ, Li SH and Wu LZ (1993). The effect of platelet activating factor on endothelial monolayer permeability by extracorporeal perfusion. *Acad. J. Sec. Mil. Med. Univ.* 14: 101-103.

Donowitz M, Ming TC and Fuster D (2013). SLC9/NHE gene family, a plasma membrane and organellar family of Na^+/H^+ exchangers. *Mol. Aspects Med.* 34: 236-251.

Lee BK and Jung YS (2012). The Na^+/H^+ exchanger-1 inhibitor cariporide prevents glutamate-induced necrotic neuronal death by inhibiting mitochondrial Ca^{2+} overload. *J. Neurosci. Res.* 90: 860-869.

Lin M, Huang X, Tan J and Wang B (2012). Adenosine alleviates hypoxia-induced rat right ventricular hypertrophy through the NHE-1/CaN signal pathway. *Nan. Fang Yi Ke Da. Xue Xue Bao* 32: 734-737.

Loo SY, Chang MK, Chua CS, Kumar AP, et al. (2012). NHE-1: a promising target for novel anti-cancer therapeutics. *Curr. Pharm. Des.* 18: 1372-1382.

Mo XG, Chen QW, Li XS, Zheng MM, et al. (2011). Suppression of NHE1 by small interfering RNA inhibits HIF-1alpha-induced angiogenesis *in vitro* via modulation of calpain activity. *Microvasc. Res.* 81: 160-168.

Montoro-García S, Shantsila E, Tapp LD, Lopez-Cuenca A, et al. (2013). Small-size circulating microparticles in acute coronary syndromes: relevance to fibrinolytic status, reparative markers and outcomes. *Atherosclerosis* 227: 313-322.

Nagata H, Che XF, Miyazawa K, Tomoda A, et al. (2011). Rapid decrease of intracellular pH associated with inhibition of Na^+/H^+ exchanger precedes apoptotic events in the MNK45 and MNK74 gastric cancer cell lines treated with 2-aminophenoxazine-3-one. *Oncol. Rep.* 25: 341-346.

Pan T, Peng S, Xu Z, Xiong B, et al. (2013). Synergetic degradation of konjac glucomannan by g-ray irradiation and hydrogen peroxide. *Carbohydr. Polym.* 2: 761-767.

Postlethwaite AE, Snyderman R and Kang AH (1976). The chemotactic attraction of human fibroblasts to a lymphocyte-derived factor. *J. Exp. Med.* 144: 1188-1203.

Sánchez Rodriguez MA, Zacarias FM, Arronte RA and Mendoza Nunez VM (2013). Effect of hormone therapy with estrogens on oxidative stress and quality of life in postmenopausal women. *Ginecol. Obstet. Mex.* 81: 11-22.

Sasahara T, Yayama K, Matsuzaki T, Tsutsui M, et al. (2013). Na^+/H^+ exchanger inhibitor induces vasorelaxation through nitric oxide production in endothelial cells via intracellular acidification-associated Ca^{2+} mobilization. *Vascul. Pharmacol.* 58: 319-325.

Vaish V and Sanyal SN (2012). Role of Sulindac and Celecoxib in chemoprevention of colorectal cancer via intrinsic pathway of apoptosis: exploring NHE-1, intracellular calcium homeostasis and Calpain 9. *Biomed. Pharmacother.* 66: 116-130.

Wan GR, Wan J, Dong XH, Li TZ, et al. (2010). The Preparative Method of a Kind of Supplement Food with the Effect of Adjusting Blood-Fat and Antagonism to Artherosclerosis. China Patent No. 201010536001.

Xiang MA, Linser PJ, Price DA and Harvey WR (2012). Localization of two Na^+- or K^+-H^+ antiporters, AgNHA1 and AgNHA2, in *Anopheles gambiae* larval Malpighian tubules and the functional expression of AgNHA2 in yeast. *J. Insect. Physiol.* 58: 570-579.

Yanamoto H, Kataoka H, Nakajo Y and Iihara K (2012). The role of the host defense system in the development of cerebral vasospasm: analogies between atherosclerosis and subarachnoid hemorrhage. *Eur. Neurol.* 68: 329-343.